



Journal of applied research and technology

ISSN: 1665-6423

UNAM, Centro de Ciencias Aplicadas y Desarrollo Tecnológico

Vats, Tanvi; Sharma, Shailesh N.

Effect of annealing temperature on the structural, morphological and optical properties of TiO₂ nanotubes and their composites with CdSe Quantum dots

Journal of applied research and technology, vol. 17, no. 2, 2019, March-April, pp. 137-148

UNAM, Centro de Ciencias Aplicadas y Desarrollo Tecnológico

DOI: <https://doi.org/10.22201/icat.16656423.2019.17.2.806>

Available in: <https://www.redalyc.org/articulo.oa?id=47471656005>

- How to cite
- Complete issue
- More information about this article
- Journal's webpage in redalyc.org

UNAM
redalyc.org

Scientific Information System Redalyc

Network of Scientific Journals from Latin America and the Caribbean, Spain and Portugal

Project academic non-profit, developed under the open access initiative



Original

Effect of annealing temperature on the structural, morphological and optical properties of TiO₂ nanotubes and their composites with CdSe Quantum dots

Tanvi Vats^{a,*}, Shailesh N. Sharma^b

^a Gautam Buddha University, Yamuna Expressway, Greater Noida-201308, India

^b National Physical Laboratory, Dr. K.S. Krishnan Marg, New Delhi- 110012, India

Abstract: In the present work we have synthesised Titanium dioxide (TiO₂) nanotubes using hydrothermal method, and studied the effect of annealing temperature on the crystallinity of the nanotubes. The nanotubes obtained were annealed at 400 °C and 600 °C. In order to elucidate the changes caused by the annealing temperature transmission electron microscopy (TEM), high resolution transmission electron microscopy (HRTEM) and X-ray diffraction (XRD) were used. The composites of titania nanotubes and CdSe quantum dots were prepared using bifunctional linker, mercaptopropionic acid. The nanocomposites were characterized using TEM and XRD. The optical properties of the modified TiO₂ nanotubes and their composites with CdSe (for potential solar cell applications) were characterized by UV-Vis absorption spectra and photoluminescence (PL) spectra.

Keywords: semiconductor oxides, nanotubes, hydrothermal, annealing, composites, optical properties

1. INTRODUCTION

Materials with nanosized structures belong to a rapid growing field of contemporary scientific interest (Kamat, 2007). Well-defined morphologies in such materials such as nanotubes, nanowire, nanotubes, and nanoparticles generally mean new physical and/or chemical properties for their bulk counterparts. It is because of the above mentioned reasons, synthesizing novel nanosized materials and probing their intrinsic properties are critical to assess their possible role in future nanodevice technology.

One-dimensional nanostructures have been in the focus of the materials science community for well more than a decade now. The extensive research in the field of one-dimensional nanostructures has led to the development of several one-dimensional moieties which can be broadly classified as carbon nanotubes and inorganic nanostructures. Carbon nanotubes in turn hold a promise to solve many challenges of materials engineering in the long run, but at present their practical applicability appears to be limited by the lack of adequately selective synthesis technologies. On the other hand, inorganic nanostructures (e.g., metallic nanowires, oxides, sulfides, selenides, etc.) can be prepared in a rather controlled manner, and therefore, their industrial scale application is very close now. TiO₂ sensitization to visible light with

* Corresponding author.

E-mail address: tanvi.vats@gmail.com (Tanvi Vats).

small nanoparticles of a low band gap semiconductor (QDs) shows several advantages, for example, high extinction coefficients, tunable energetic levels and multiple exciton generation effects (Burda, Chen, Narayanan, & El-Sayed, 2005; Fernandes et al., 2016; Gulati, Santos, Findlay, & Losic, 2015; Grätzel, 2001; Hernández-Martínez, Estevez, Vargas, Quintanilla, & Rodríguez, 2012; Horváth, Kukovecz, Kónya, & Kiricsi, 2007; Hoyer, 1996; Ou & Lo, 2007). Despite of the great promise the dream of a highly efficient quantum dot /conducting polymer sensitized solar cell is still elusive. Undesirable loss of electrons at grain boundaries via recombination with redox couples impedes the efficient transport of electrons to collecting electrode surface. Titania nanotubular structures, in particular, hold special promise for many of these same applications due to their high length/diameter aspect ratio, which allows them to meet the requirements of high surface area and reduced interfacial boundaries.

In the present work we have synthesised TiO_2 nanotubes using hydrothermal method, and studied the effect of annealing temperature on the crystallinity of the nanotubes. Varying the annealing temperature is one strategy to induce change in the morphological properties of materials. Annealing transforms the as-deposited amorphous titanium oxide phase to polycrystalline anatase TiO_2 . It has been shown that altering the annealing conditions can affect the crystal structure and photoresponse of the TiO_2 NTs (Zhu, Neale, Miedaner, & Frank, 2007).

The nanotubes so obtained were sensitised using CdSe quantum dots and the structural, morphological, optical and electrical aspects have been studied.

2. MATERIAL AND METHODS

2.1 MATERIALS

For synthesis of titania nanotubes TiO_2 powder (Central Drug House, 99.5%), NaOH (Merck, 98%), HCl (Merck, 35%) were used as received. The precursors cadmium oxide (CdO, Aldrich, 99.99% purity), tetradecylphosphonic acid (TDPA, Alfa Aesar, 98% purity), trioctylphosphine oxide (TOPO, Aldrich, 99% purity), selenium (Aldrich, 99.5% purity), and trioctylphosphine (TOP, Aldrich, 90% purity) Oleic acid (OA, Central Drug House, 95% purity) were used as supplied to prepare CdSe QDs. Mercaptopropionic

acid (MPA, Sigma Aldrich, >99%), acetonitrile (SRL, extrapure AR, 99.5% purity) and Sulphuric Acid (Sigma Aldrich, 99.9% purity) were used to prepare linker solution.

2.2 METHODS

(a) Synthesis of TiO_2 nanotubes

Hydrothermal has been a very common method used to prepare TiO_2 nanotubes since it was developed by Kasuga and co-workers (Kasuga, Hiramatsu, Hoson, Sekino, & Niihara, 1998, 1999; Wang et al, 2002). In the typical synthesis TiO_2 powder was annealed at 400°C and was stirred with 10M NaOH in an autoclave at 130°C for 24 hrs. The treated powder was washed with dilute HCl and distilled water and separated by centrifugation. The nanotubes so obtained were annealed in two batches at 400°C and 600°C and their composition was analysed using XRD.

(b) Sensitization of TNT with CdSe Quantum Dots

The synthesis of CdSe nanoparticles were carried out by the chemical route using TOPO as a capping agent to control the growth of the nanoparticles to desired sizes, whose details can be found elsewhere (Bavykin, Parmon, Lapkin, & Walsh, 2004; Sharma et al, 2007). The titania nanotubes were sensitised with CdSe quantum dots by the aid of bifunctional linker mercaptopropionic acid in the similar manner as described in our previously reported work (Sharma, Sharma, Singh, & Shivaprasad, 2007). In brief the TiO_2 moieties were immersed in 1M solution of mercaptopropionic acid solution for 24 hour and then were gradually added to CdSe solution. The choice of the linker stemmed from the fact that it possesses a thiol group (-SH) that links to the CdSe quantum dots via Cd-S bond, and another carboxylic acid group (-COOH) that links to the TiO_2 . It is known that the selection of the linker for the better anchorage of colloidal QD's on to the TiO_2 surface plays a vital role in the performance of QDSSC's in determining the efficiency of electron injection into the matrix.

2.3 INSTRUMENTATION

The crystalline phases of the products were determined by X-ray powder diffraction by using a Rigakuminiflex II diffractometer with Cu K alpha radiation (λ) 1.54 Å. The morphologies of the samples were studied via a Scanning Electron Microscopy (SEM, Zies EVO M810 variable pressure SEM). Microstructural properties

were obtained using a transmission electron microscope (TEM), JEOL make model JEM-200CX. For the TEM observations, the powders were dispersed in 2-propanol and ultrasonicated for 15 min. A few drops of this ultrasonicated solution were taken on a carbon-coated copper grid. Compositional analysis was performed by energy dispersive X-ray analysis (EDAX) used with the SEM. Optical absorbance of the samples was recorded via a UV-vis-NIR spectrophotometer Shimadzu 3101 spectrometer. The PL was measured using a home assembled system consisting of a two stage monochromator, a photomultiplier tube (PMT) with a lock-in amplifier for PL detection, and an Ar⁺ ion laser operating at 488 nm and 5 mW (corresponding to 0.125 W cm⁻²) for excitation in all the measurements. X-ray photoelectron spectroscopy (XPS) measurements were performed in an ultra-high vacuum chamber (PHI 1257) with a base pressure of $\sim 4 \times 10^{-10}$ torr. The pressure during data acquisition and argon ion etching is of the order of 2.5×10^{-7} torr. The XPS spectrometer is equipped with a high precision sample manipulator, MgK α (1253.6 eV) X-ray anode, a high-resolution hemispherical analyzer (25 meV) and a 0 – 5 keV differentially pumped Ar⁺ ion gun. Survey scans and core level XPS spectra were obtained using pass energies of 100 and 40 eV, respectively. The resolution of the acquired core level spectra is 0.1 eV, at 90% of the peak height. The data obtained was deconvoluted into their Gaussian components, using standard FWHM and position values of the known valence states (Sharma, Vats, Kumar, Jain, & Narula, 2011). All the data were corrected for electrostatic charging using the XPS lines of the graphitic C (1s) as internal energy reference.

3. RESULTS AND DISCUSSIONS

The formation mechanism of TNT has been proposed to follow a 3D \rightarrow 2D \rightarrow 1D approach. This suggests that the raw TiO₂ powder first convert to lamellar structures which then roll up to form tubes. The raw TiO₂ material is treated with NaOH aqueous solution, Ti–O–Na and Ti–OH bonds are formed after some of the Ti–O–Ti bonds are broken.

The Ti–O–Na and Ti–OH bonds are believed to react with acid and water to form new Ti–O–Ti bonds when the material is treated with HCl aqueous solution and distilled water.

The titania nanotubes are formed in the stage of the acid treatment following the alkali treatment. The Ti–OH bond may form a sheet, which is contained in the tube structure. The Ti–O–Ti bonds or Ti–O–H–O–Ti hydrogen bonds are generated through the dehydration of Ti–OH bonds by HCl aqueous solution, the bond distance from one Ti to the next Ti on the surface decreases, resulting in the folding of the sheets. During this process, a slight, residual electrostatic repulsion due to Ti–O–Na bonds may lead to connection between the ends of the sheets and thus the completion of a tube structure. Bavykin and co-workers suggested that the driving force for curving of the sheets arose from asymmetry due to, e.g., preferential doping of the sheets with sodium or hydrogen (e.g., hydrogen deficient H₂Ti₃O₇) together with unsymmetrical surface forces due to locally high surface energy during the crystallisation/dissolution (Fu, Liu, & Shen, 2014; Kasuga et al, 1999; Wang, Hu, Duan, Sun, & Xue, 2002). This approach can be explained in the following schematic (fig. 1).

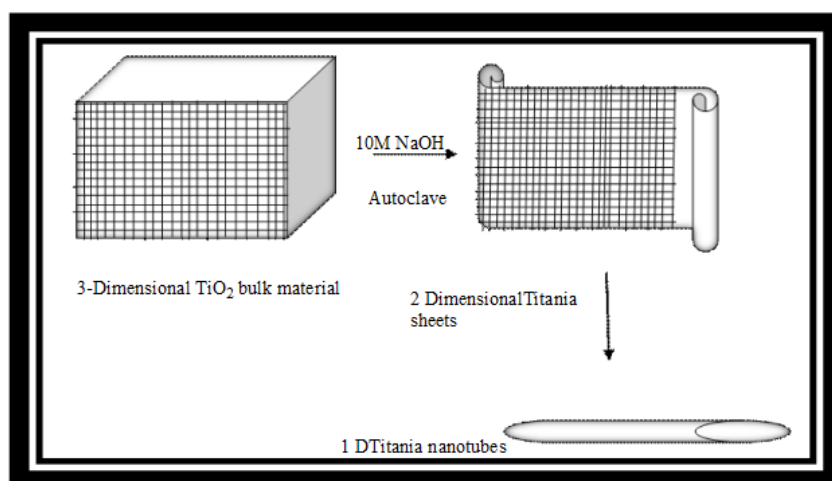


Fig. 1. Diagrammatic representation explaining the process of nanotube formation.

(a) X-Ray diffraction Pattern

Figure 2 (a & b) shows the XRD pattern of TiO₂ nanotubes and nanoparticles. In nanotubes sample rutile peaks are indexed with R while A peaks refer to the anatase planes.

The phase composition is estimated using the Spurr equation (Zhu et al., 2007):

$$F_A = 100 - \left[\frac{1}{1 + 0.8 \left(\frac{I_{A(101)}}{I_{R(110)}} \right)} \right] 100 \quad (1)$$

where, F_A is the mass fraction of anatase in the sample and I_A and I_R are the integrated intensities of the main peaks of anatase (101) and rutile (110), respectively. From the above equation the percentage of anatase phase is 51.92% for the sample annealed at 400°C and 45.36% for the sample annealed at 600°C.

Fig. 2 (c & d) give the XRD pattern of CdSe -TNT nanocomposites. The pattern consists of the main TNT peaks along with CdSe features. The dense contrast indicates the presence of amorphous CdSe. The difference between the XRD pattern of TNT, CdSe and the nanocomposites suggest the formation of a heterostructure.

The XRD pattern along with TEM, HRTEH and EDAX analysis give the signatures of formation of nanocomposite.

(b) SEM studies

Fig. 3 gives the SEM images of TiO₂ nanotubes annealed at 600°C. The image shows randomly arranged nanotubes which is a characteristic of hydrothermal synthesis. Also some spherical particles are observed which depict the unconverted powder. The encircled portion gives the image of a high aspect ratio single nanotube almost 150nm long.

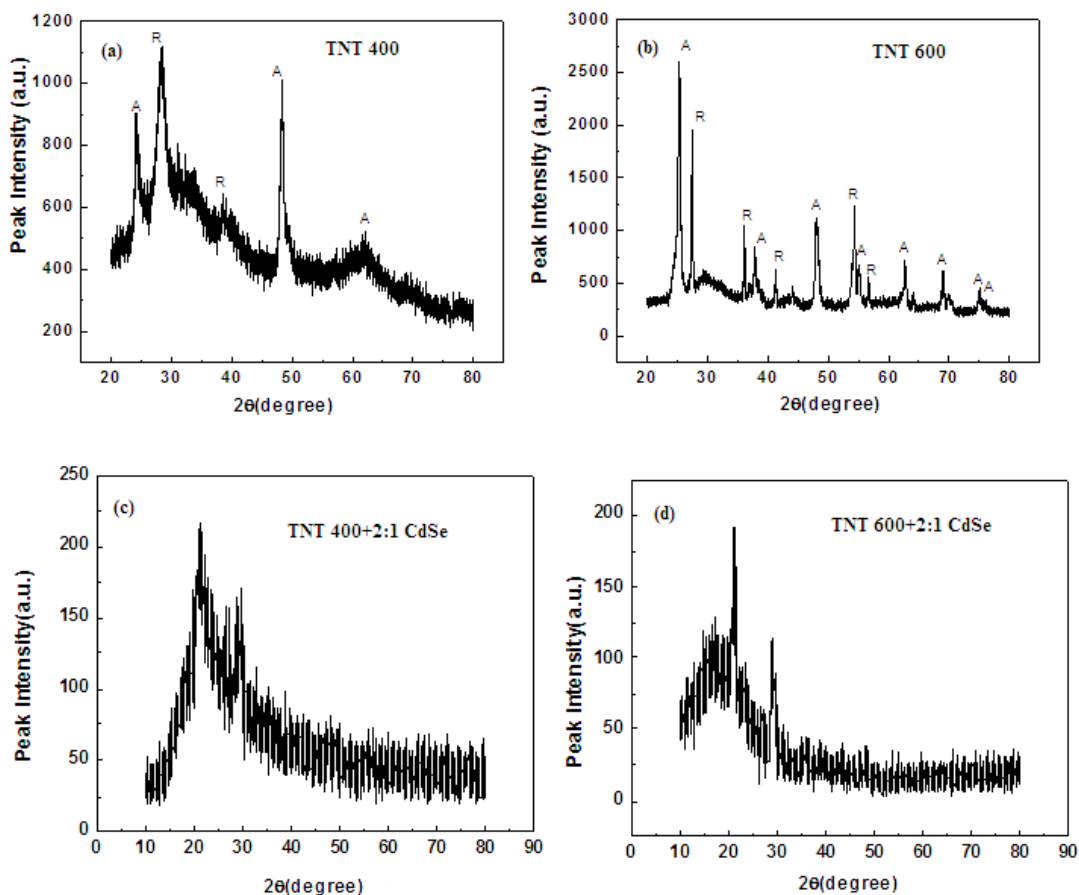


Fig. 2. XRD pattern of (a) titania nanotubes annealed at 400 (b) titania nanotubes annealed at 600°C (c) CdSe- titania nanotubes nanocomposites (titania nanotubes) annealed at 400°C (d) CdSe- titania nanotubes nanocomposites (titania nanotubes) annealed at 600°C.

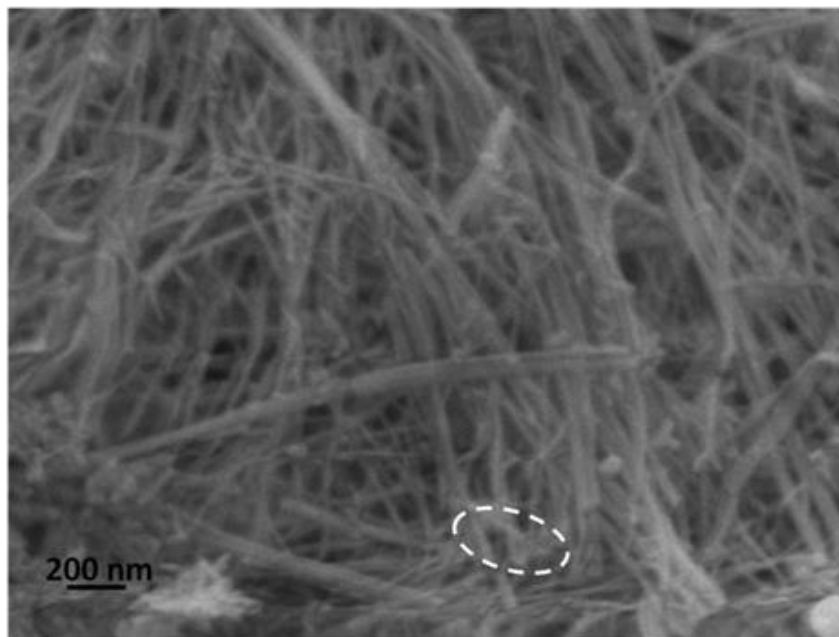


Fig. 3. SEM images of titania nanotubes.

(c) TEM, HRTEM and EDAX

Fig. 4 shows the TEM image of the nanotubes. The images reveal high aspect ratio of the nanotubes with almost 120-150 nm length and about 20 nm in diameter. The nanotubes are randomly aligned indicating the use of hydrothermal route for the nanotube formation. The inset in the figure shows the high resolution image of a nanotube inclined horizontally. The electron diffraction pattern comprising of concentric rings indicates the polycrystalline nature of the nanotubes. The carbon and copper signals are due to the carbon coated copper grids. Fig. 5 and Fig. 6 give the TEM of CdSe-TNT nanocomposites with nanotubes annealed at 400 and 600°C respectively. The nanotubes clearly appear as hollow tubular structures while the amorphous CdSe QDs present a featureless dark contrast. One of the major differences between the two nanocomposites is the amount of QD coverage in both the cases. The TEM images indicate greater QD coverage in the samples annealed at 600°C. This could be attributed to the greater anatase content of the samples. The emission pattern also gives a greater quenching in these samples. The encircled portion in Fig. 5 (a) is the nanocomposites formed. The distinct difference in the spacing of lattice fringes in the HRTEM (Fig. 5(b), Fig. 6(b)) pattern is the signature of the nanocomposite formation. The electron diffraction pattern (Fig. 5(c), Fig. 6(c)) consisting of concentric rings is indicative of high crystalline nature of the samples.

Fig. 7 gives the EDAX of the titania nanotubes. The carbon and copper signals are due to the carbon coated copper grids. The EDAX pattern confirms the formation of TiO_2 . Fig. 8(b) and (c) give the EDAX of the CdSe-TNT nanocomposites. It is imperative to note the presence of sulphur peaks in the EDAX pattern apart from the Ti, O, C, Cd, Se peaks. The sulphur peaks are indicative of the use of mercaptopropionic acid (MPA) as a bifunctional linker molecule.

(d) Absorption Studies

Fig. 9 gives the comparative absorption pattern of TNT annealed at 600°C, TNT annealed at 400°C and their nanocomposites with CdSe.

The absorption spectrum for titania nanotubes is observed as a broad peak giving two features one at 232 nm and another at 260 nm. This hints at the presence of mixed phases of TiO_2 . The position of these peaks does not change on changing the annealing temperature. However, the peak observed is sharper for the nanotubes at 600°C. The absorption spectra of the nanocomposites are an overlap of the spectrum of individual components i.e., TiO_2 feature at 232 nm and 260 nm while CdSe feature at around 320 nm. However, the CdSe peaks are more pronounced in the hybrids with nanotubes annealed at 400°C (Bavykin, Gordeev, Moskalenko, Lapkin, & Walsh, 2005).

(e) Photoluminescence Studies

PL spectra of CdSe showed a constant decrease in intensity on the gradual addition of TNT indicating

(e) Photo luminescence Studies

PL spectra of CdSe showed a constant decrease in intensity on the gradual addition of TNT indicating charge transfer Fig. 10. In case of TNT annealed-annealed at 600°C after reaching a certain point no further decrease was observed indicating saturation. However, an interesting feature was observed in case of TNT annealed-annealed at 400°C, the PL peak started increasing in intensity and after certain concentration it became greater than the original peak. This phenomenon has been reported in the systems containing titania nanotubes – conducting polymer (Nguyen, Martini, Liu, & Schwartz, 2000; Verma, Rao, & Dutta, 2009). The phenomenon has been explained due to the transfer of photogenerated electrons to the TNT (Padmanabhan et al., 2007; Vijayan, Dimitrijevic, Rajh, & Gray, 2010).

In the simplest case of collisional quenching, the

following relation, called the Stern–Volmer equation [2] holds:

$$I_0/I = 1 + K_{SV}[Q] \quad (2)$$

where I_0 and I are the fluorescence intensities observed in the absence and presence, respectively of quencher, $[Q]$ is the quencher concentration and K_{SV} is the Stern–Volmer quenching constant. From the linear portion of Stern–Volmer plots (fig. 11) K_{SV} is calculated which comes out to be 0.4×10^{-2} in case of TNT annealed at 400°C while 0.8×10^{-2} in case of TNT annealed annealed at 600°C indicating a faster charge transfer kinetics in spherical particles which is accounted to the higher crystallinity. However the quenching saturation is observed at lower TNT concentration for TNT annealed annealed at 400°C owing to higher anatase content.

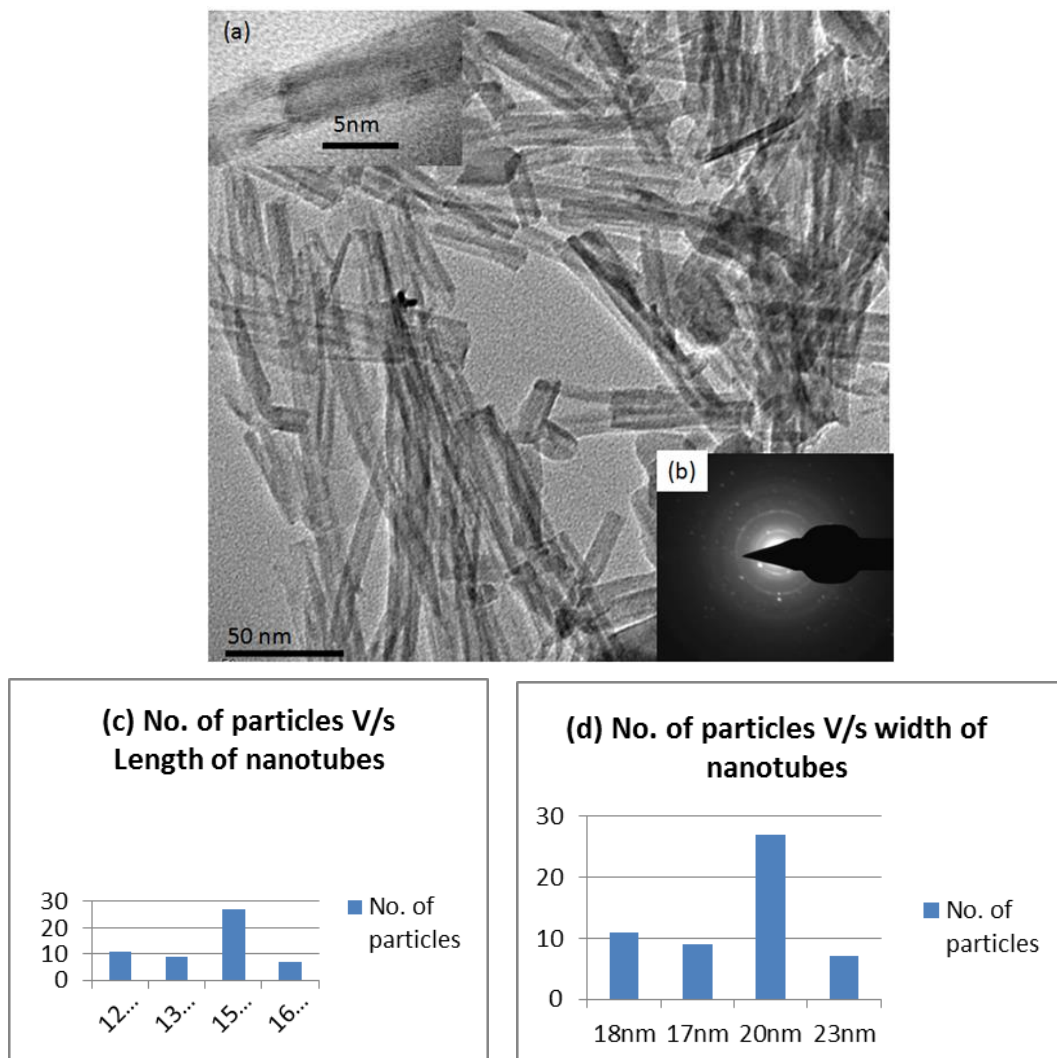


Fig. 4. TEM image of titania nanotubes. Inset (a) HRTEM of single nanotube. (b) Electron diffraction pattern (c) Frequency distribution of length (d) Frequency distribution of width.

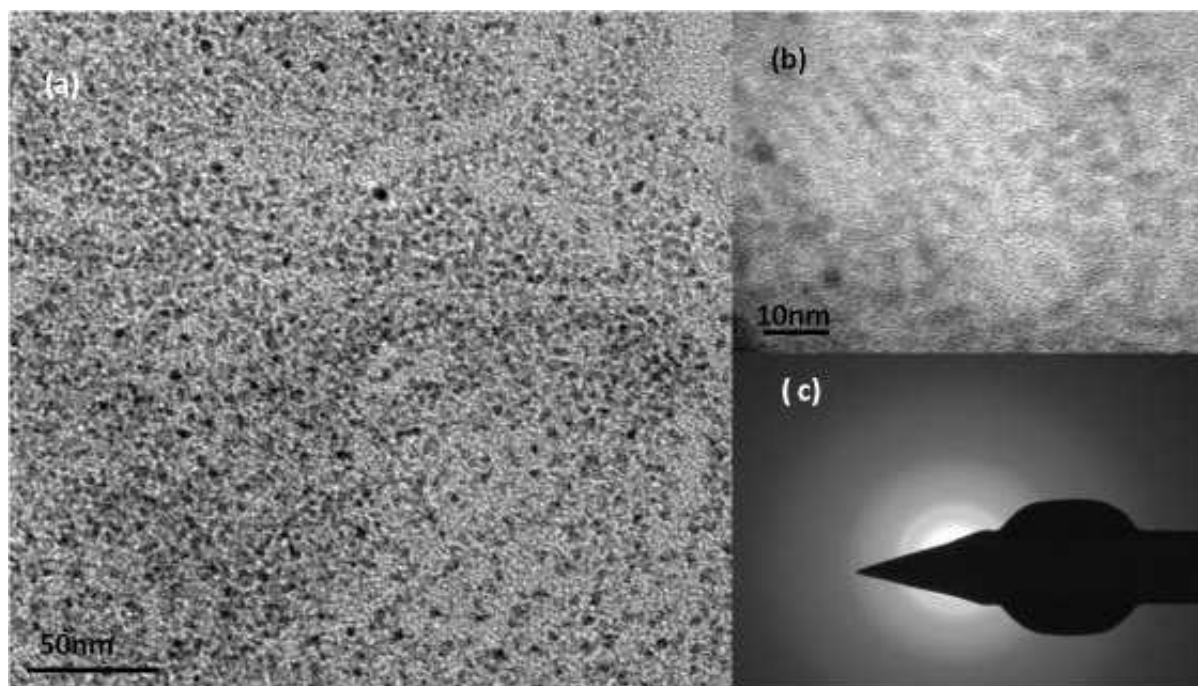


Fig. 5. TEM image of CdSe quantum dots.

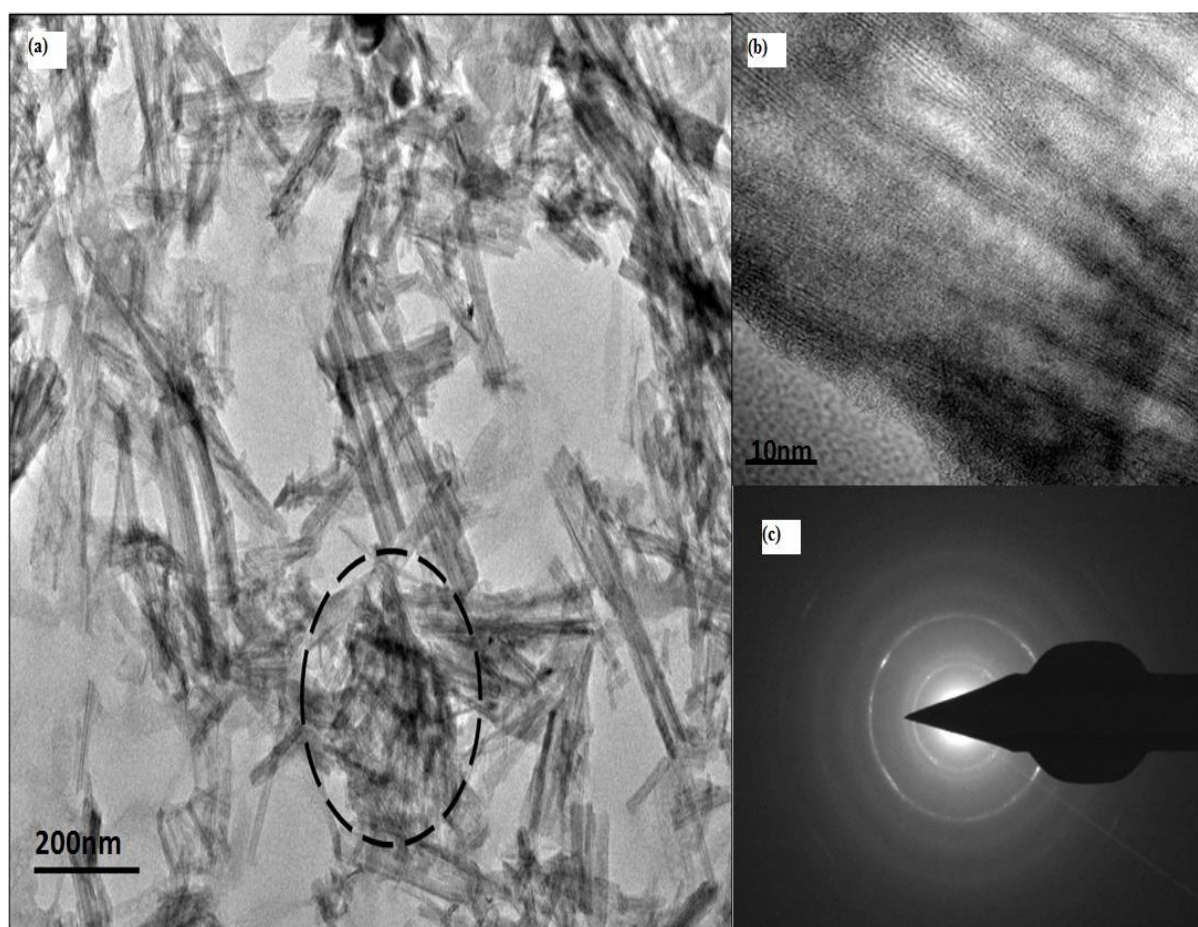


Fig. 6. (a) TEM CdSe- titania nanotubes nanocomposites (titania nanotubes) annealed at 400°C. (b)HRTEM and (c) electron diffraction pattern of the samples.

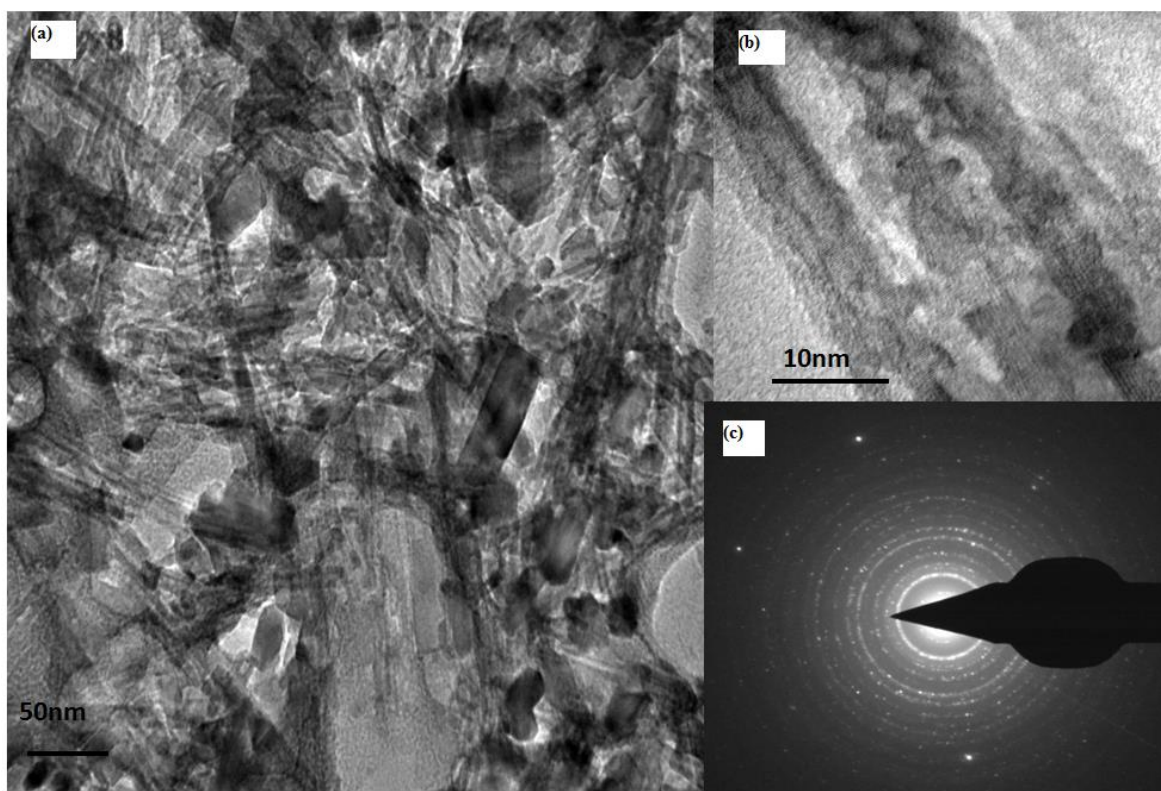


Fig. 7. (a) TEM images CdSe- titania nanotubes nanocomposites (titania nanotubes) annealed at 600°C. (b)HRTEM and (c) electron diffraction pattern of the samples.

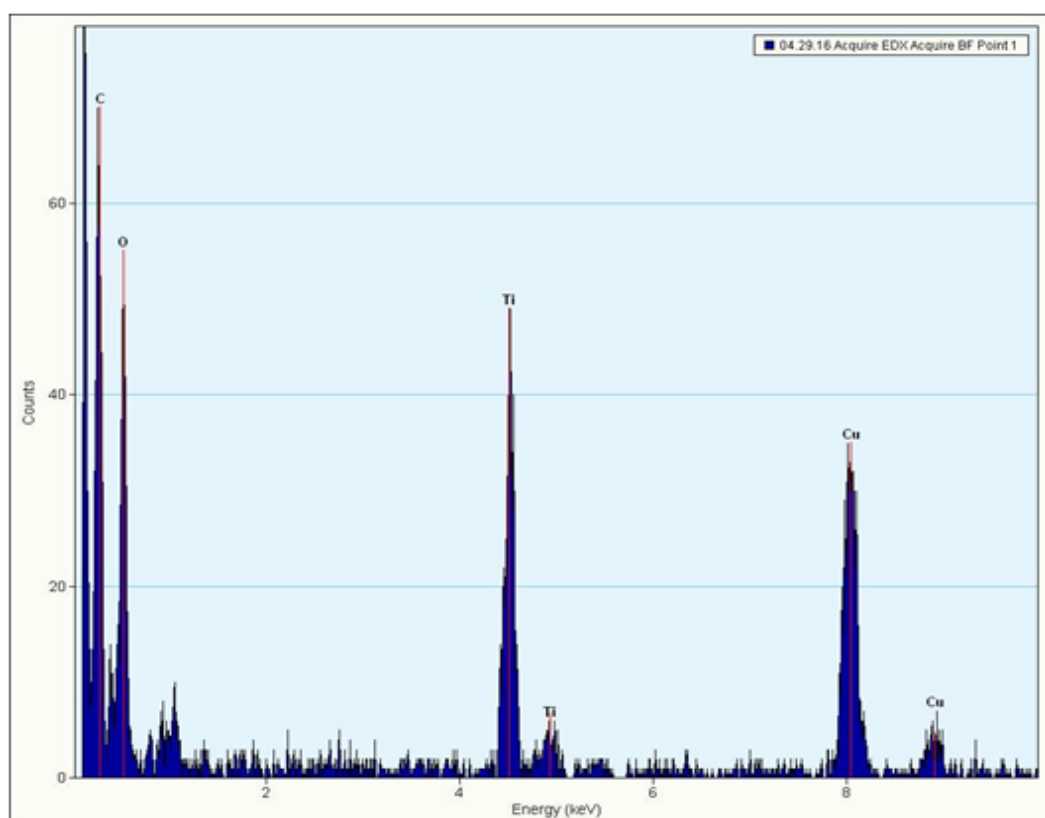


Fig. 8. EDAX pattern of titania nanotubes.

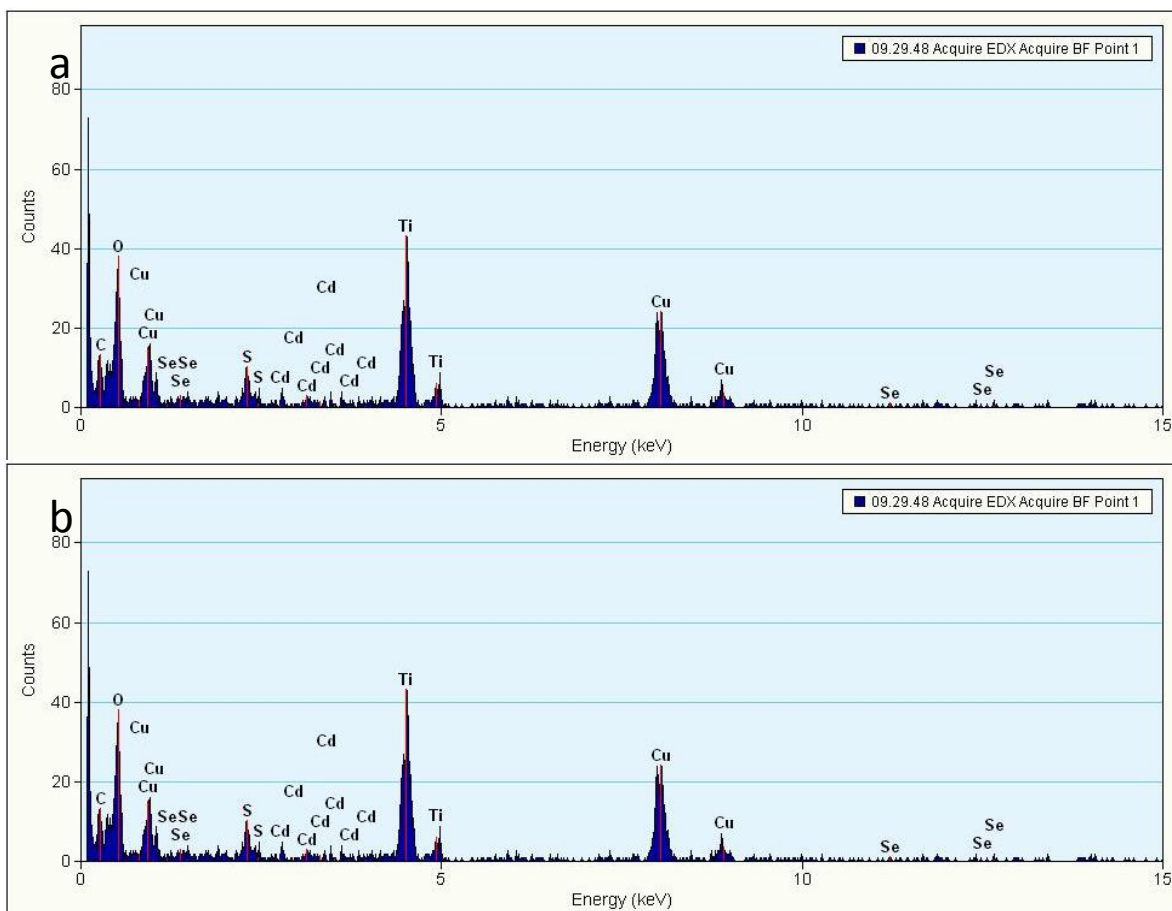


Fig. 9. EDAX pattern of (a) CdSe- titania nanotubes nanocomposites (titania nanotubes) annealed at 400°C (b) CdSe- titania nanotubes nanocomposites (titania nanotubes) annealed at 600°C.

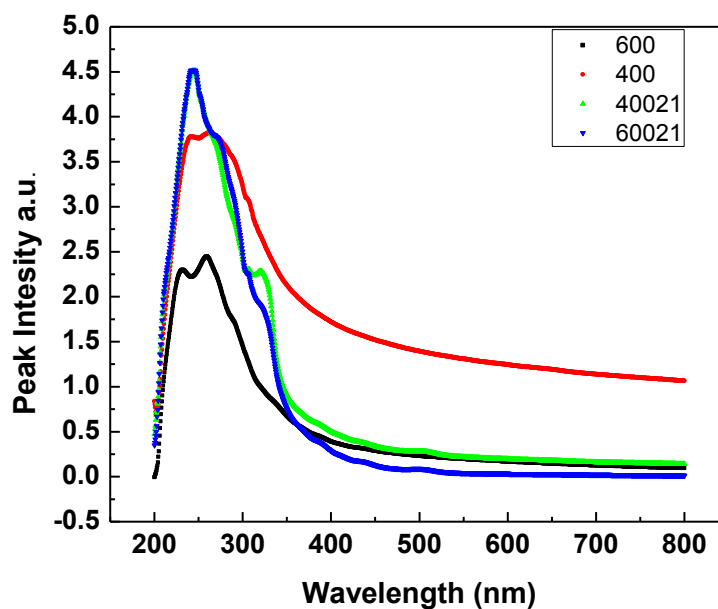


Fig. 10. Absorption spectra of (a) titania nanotubes annealed at 400 (b) titania nanotubes annealed at 600°C (c) CdSe- titania nanotubes nanocomposites (titania nanotubes) annealed at 400°C (d) CdSe- titania nanotubes nanocomposites (titania nanotubes) annealed at 600°C.

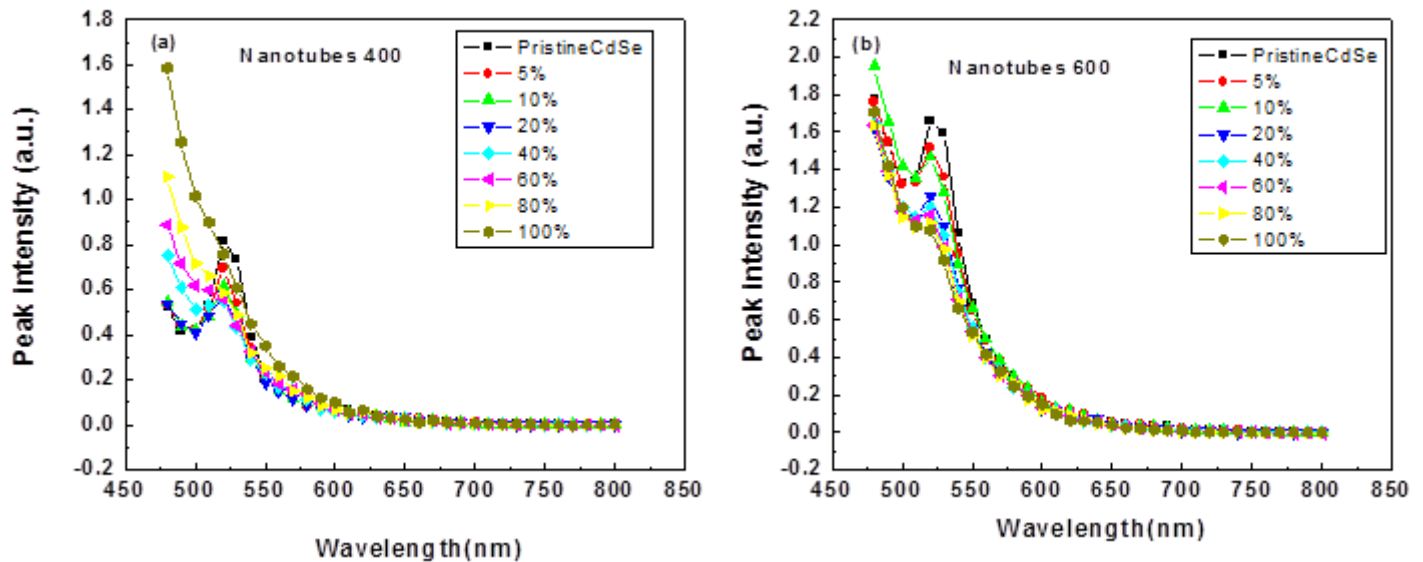


Fig. 11. PL emission of (a) CdSe- titania nanotubes nanocomposites (titania nanotubes) annealed at 400°C (b) CdSe- titania nanotubes nanocomposites (titania nanotubes) annealed at 600°C. The numbers indicate the percentage by weight.

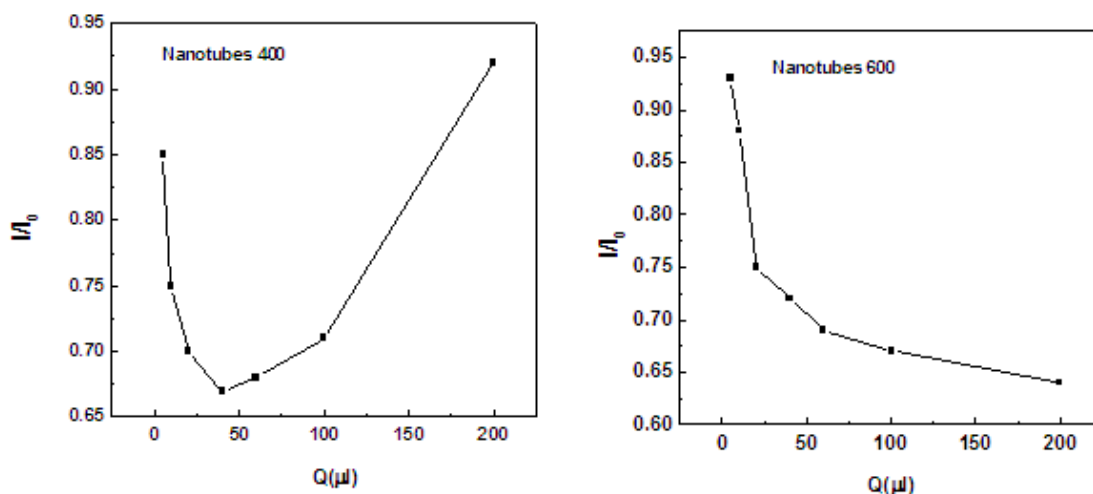


Fig. 12. Stern-Volmer plots (a) CdSe- titania nanotubes nanocomposites (titania nanotubes) annealed at 400°C (b) CdSe- titania nanotubes nanocomposites (titania nanotubes) annealed at 600°C.

4. CONCLUSION

TiO₂ nanotubes were successfully synthesised using hydrothermal method. The experimental procedure includes thermal treatment of TNT arrays in air. This process strongly alters the morphology of the individual NTs and has been proved to be highly effective in inducing crystallinity and increasing charge transfer properties, which, in turn, significantly affects the electron transport and recombination kinetics and the solar energy conversion properties of QDSSCs and BHJs.

Photoluminescence quenching data indicate that altering the microstructure changes the dynamics of transport and recombination in different ways. The Stern-Volmer plots give faster quenching kinetics of TNT annealed at 600°C, while those annealed at 400 °C quenched the PL intensity at lower concentration. The study indicates that the one dimensional nanotubular TiO₂ holds a special promise to be a useful photovoltaic material due to its high length/diameter aspect ratio, which allows them to meet the requirements of high surface area and reduced

interfacial boundaries. Understanding the fundamentals of the structural parameters, methods by which these parameters can be altered and exploiting them to build devices with high efficiency hold the key to the energy crisis of the world.

ACKNOWLEDGEMENT

The authors thank National Physical Laboratory, New Delhi, India for the valuable financial contribution and support in this study.

CONFLICT OF INTEREST

The authors have no conflicts of interest to declare.

REFERENCES

- Bavykin, D. V., Gordeev, S. N., Moskalenko, A. V., Lapkin, A. A., & Walsh, F. C. (2005). Apparent two-dimensional behavior of TiO₂ nanotubes revealed by light absorption and luminescence. *The Journal of Physical Chemistry B*, 109(18), 8565–8569.
- Bavykin, D. V., Parmon, V. N., Lapkin, A. A., & Walsh, F. C. (2004). The effect of hydrothermal conditions on the mesoporous structure of TiO₂ nanotubes. *Journal of Materials Chemistry*, 14(22), 3370–3377.
- Burda, C., Chen, X., Narayanan, R., & El-Sayed, M. A. (2005). Chemistry and properties of nanocrystals of different shapes. *Chemical reviews*, 105(4), 1025–1102.
- Fernandes, J. A., Khan, S., Baum, F., Kohlrausch, E. C., Dos Santos, J. A. L., Baptista, D. L., ... & Santos, M. J. L. (2016). Synergizing nanocomposites of CdSe/TiO₂ nanotubes for improved photoelectrochemical activity via thermal treatment. *Dalton Transactions*, 45(24), 9925–9931.
- Grätzel, M. (2001). Photoelectrochemical cells. *Nature*, 414(6861), 338–344.
- Gulati, K., Santos, A., Findlay, D., & Losic, D. (2015). Optimizing anodization conditions for the growth of titania nanotubes on curved surfaces. *The Journal of Physical Chemistry C*, 119(28), 16033–16045.
- Fu, H., Liu, H., & Shen, W. (2014). A composite CdS thin film/TiO₂ nanotube structure by ultrafast successive electrochemical deposition toward photovoltaic application. *Nanoscale research letters*, 9(1), 631.
- Hernández-Martínez, A. R., Estevez, M., Vargas, S., Quintanilla, F., Rodríguez, R. (2012). Natural pigment-based dye-sensitized solar cells *Journal of Applied Research and Technology* 10(1), 38–47.
- Horváth, E., Kukovecz, Á., Kónya, Z., & Kiricsi, I. (2007). Hydrothermal conversion of self-assembled titanate nanotubes into nanowires in a revolving autoclave. *Chemistry of materials*, 19(4), 927–931.
- Hoyer, P. (1996). Formation of a titanium dioxide nanotube array. *Langmuir*, 12(6), 1411–1413.
- Kamat, P. V. (2007). Meeting the clean energy demand: nanostructure architectures for solar energy conversion. *The Journal of Physical Chemistry C*, 111(7), 2834–2860.
- Kasuga, T., Hiramatsu, M., Hoson, A., Sekino, T., & Niihara, K. (1998). Formation of titanium oxide nanotube. *Langmuir*, 14(12), 3160–3163.
- Kasuga, T., Hiramatsu, M., Hoson, A., Sekino, T., & Niihara, K. (1999). Titania nanotubes prepared by chemical processing. *Advanced Materials*, 11(15), 1307–1311.
- Nguyen, T. Q., Martini, I. B., Liu, J., & Schwartz, B. J. (2000). Controlling interchain interactions in conjugated polymers: the effects of chain morphology on exciton–exciton annihilation and aggregation in MEH–PPV films. *The Journal of Physical Chemistry B*, 104(2), 237–255.
- Ou, H. H., & Lo, S. L. (2007). Review of titania nanotubes synthesized via the hydrothermal treatment: Fabrication, modification, and application. *Separation and Purification Technology*, 58(1), 179–191.
- Padmanabhan, S. C., Pillai, S. C., Colreavy, J., Balakrishnan, S., McCormack, D. E., Perova, T. S., ... & Kelly, J. M. (2007). A simple sol–gel processing for the development of high-temperature stable photoactive anatase titania. *Chemistry of Materials*, 19(18), 4474–4481.
- Sharma, H., Sharma, S. N., Singh, S., Kishore, R., Singh, G., & Shivaprasad, S. M. (2007). Surface sensitive probe of the morphological and structural aspects of CdSe core–shell nanoparticles. *Applied surface science*, 253(12), 5325–5333.
- Sharma, H., Sharma, S. N., Singh, G., & Shivaprasad, S. M. (2007). Effect of oxidation induced surface state formation on the properties of colloidal CdSe quantum dots. *Journal of nanoscience and nanotechnology*, 7(6), 1953–1959.
- Sharma, S. N., Vats, T., Kumar, M., Jain, K., & Narula, A. K. (2011). Probing the compositional, structural and morphological aspects of CdSe–TiO₂ nanocomposites by surface-sensitive techniques. *Materials Science and Engineering: B*, 176(17), 1342–1348.
- Verma, D., Rao, A. R., & Dutta, V. (2009). Surfactant-free CdTe nanoparticles mixed MEH–PPV hybrid solar cell deposited by spin coating technique. *Solar Energy Materials and Solar Cells*, 93(9), 1482–1487.
- Vijayan, B., Dimitrijevic, N. M., Rajh, T., & Gray, K. (2010). Effect of calcination temperature on the photocatalytic reduction and oxidation processes of hydrothermally synthesized titania nanotubes. *The Journal of Physical Chemistry C*, 114(30), 12994–13002.

- Wang, Y. Q., Hu, G. Q., Duan, X. F., Sun, H. L., & Xue, Q. K. (2002). Microstructure and formation mechanism of titanium dioxide nanotubes. *Chemical Physics Letters*, 365(5), 427-431.
- Zhu, K., Neale, N. R., Miedaner, A., & Frank, A. J. (2007). Enhanced charge-collection efficiencies and light scattering in dye-sensitized solar cells using oriented TiO₂ nanotubes arrays. *Nano letters*, 7(1), 69-74.